



# Alongshore sediment transport analysis for a semi-enclosed basin: a case study of the Gulf of Riga, the Baltic Sea

Tarmo Soomere<sup>1,2</sup>, Mikolaj Zbiegniew Jankowski<sup>1</sup>, Maris Eelsalu<sup>1</sup>, Kevin Ellis Parnell<sup>1</sup>, Maija Viška<sup>3</sup>

<sup>1</sup>Department of Cybernetics, School of Science, Tallinn University of Technology, Tallinn, 19086 Estonia

5 <sup>2</sup>Estonian Academy of Sciences, Kohtu 6, Tallinn, 10130 Estonia

<sup>3</sup>Latvian Institute of Aquatic Ecology, Rīga, LV-1007 Latvia

*Correspondence to:* Tarmo Soomere (tarmo.soomere@taltech.ee)

**Abstract.** The properties of wave-driven sediment transport and the dimensions of single sedimentary compartments are often radically different in different parts of semi-enclosed water bodies with an anisotropic wind climate. The western, southern and eastern shores of the Gulf of Riga are a remote part of the more than 700 km long interconnected sedimentary coastal system of the eastern Baltic Sea from Samland in Kaliningrad District, Russia, to Pärnu Bay, Estonia. Even though shores of the gulf are generally straight or gently curved, the presence of small headlands and variations in the orientation of the coastline give rise to numerous fully or partially separated sedimentary compartments. We decompose sedimentary shores of this gulf into single compartments and cells based on the analysis of wave-driven potential sediment transport using high-resolution wave time series and the Coastal Engineering Research Centre (CERC) approach. The western shores of the Gulf of Riga form a large interconnected sedimentary system with intense sediment transport that is largely fed by sand transported from the Baltic proper. The southern shores have much less intense sediment transport and mostly accumulation areas. The south-eastern sector of the gulf is an end station of counter-clockwise sand transport. The eastern shore consists of several almost isolated sedimentary cells and contains a longer segment where clockwise transport predominates. The transport rates along different shore segments show extensive interannual variations but no explicit trends in the period 1990–2022.

## 1 Introduction

Wave-driven sediment transport in the surf zone is a core process that shapes the shores of seas and oceans, including the key drivers of beach profile change, functioning of the cut and fill cycle, and loss of sediment to the offshore via driving surf zone turbulence (Aagaard et al., 2021). It is also the principal agent of coastal erosion, alongshore sediment transport and sediment accumulation in the vicinity of the shoreline. These processes can be unidirectional, or circulatory on comparatively straight open ocean shores where waves usually approach the shore from a specific direction or at a small angle and where major headlands commonly divide the sedimentary system into large cells and extensive compartments (Thom et al., 2018).



30 The situation is complicated in water bodies of complex shape, such as the Baltic Sea (Fig. 1) where waves often approach the shore at large angles (Soomere and Viška, 2014; Eelsalu et al., 2024a; Soomere et al., 2024). The interplay of a high angle of approach and wind patterns with multi-peak directional structure gives rise to exceptionally powerful alongshore sediment flux (Viška and Soomere, 2013b) under a fairly modest wave climate (Björkqvist et al., 2018; Giudici et al., 2023), specific mechanisms that stabilise almost equilibrium beaches (Eelsalu et al., 2022), and persistent divergence areas at certain locations with small changes in the orientation of the coastline (Soomere and Viška, 2014; Eelsalu et al., 2023). To better characterise such situations, we use the term “cell” to denote relatively small coastal segments, elementary sedimentary units that are either mostly separated from the neighbouring segments or exhibit other clearly identifiable features (e.g., cells of predominantly one-directional sediment transit versus cells with almost no net sediment transport). In a similar manner, we use the term “compartment” to denote clusters of cells that usually exchange sediment within the cluster but have either very limited sediment exchange with other compartments (e.g., because of the presence of a major divergence area of sediment flux), or only one-way sediment exchange with a neighbour.

Massive alongshore sediment transport is one of the main reasons for extensive coastal erosion (Eberhards et al., 2009) and the formation of large accumulation features that sometimes occur at a large distance from the erosion areas in the eastern Baltic Sea (Tönisson et al., 2016). This transport may amplify the impact of coastal defence structures on sediment deficit (Bernatchez and Fraser, 2012). It can also be a major problem from the viewpoint of coastal infrastructure design and maintenance (Bulleri and Chapman, 2010), the management of urban coastal landscape and for increasing resilience of coastal socio-ecological systems (Villasante et al., 2023). Persistent sediment flux divergence areas may serve as invisible barriers to alongshore sediment transport and split large seemingly connected sedimentary systems into smaller cells and compartments. Separation of large sedimentary systems into smaller cells makes it possible to greatly simplify the analysis of properties of the entire system (Kinsela et al., 2017), better understand the functioning and resilience of single compartments, and reach optimum solutions for the design of various structures or beach management and nourishment actions as demonstrated, e.g., in Cappucci et al. (2020) and Susilowati et al. (2022). Moreover, such divergence areas are natural limits for the propagation of pollution that is carried along the shore with sediment parcels.

Wave-driven sediment transport plays a particularly large role in shaping sedimentary and/or easily erodible shores of relatively young water bodies, such as the Baltic Sea (Fig. 1). Wave impact is almost negligible for the development of its western, northern and north-eastern bedrock coasts that have very little sandy coast. The other shores of this sea, from southern Sweden counter-clockwise to the vicinity of Saint Petersburg is predominantly sedimentary, most of which is still rapidly developing (Harff et al., 2017). The coastal stretch from the Sambian Peninsula (Samland) to Pärnu Bay in the Gulf of Riga is a >700 km long interconnected sedimentary coastal system, with an almost continuous strip of sand and mostly counter-clockwise sediment transport (Knaps, 1966; see Viška and Soomere, 2013b for references). This transport is particularly massive along the north-western shore of Latvia where it reaches  $1,000,000 \text{ m}^3 \text{ yr}^{-1}$  (Knaps, 1966).

Wave-driven transport along this stretch of coast has been estimated at a relatively low resolution of about 5.5 km (Viška and Soomere, 2013b; Soomere and Viška, 2014). There is one major accumulation area near Cape Kolka (north-western

Latvia) and one almost complete sediment flux divergence area near Cape Akmenrags on the western coast of Latvia, the result of an interplay of the shape of this stretch of coast and the two predominant wind directions in the area (Soomere, 2003).

These features divide this sedimentary system into three major compartments. Two of them are weakly interconnected with potential annual net sediment flux across Cape Akmenrags occurring approximately once in 40 yr (Soomere and Viška, 2014) and an area with sediment transport from the Baltic proper shores to the interior of the Gulf of Riga which apparently is almost entirely one-way. The resolution, however, is too low to identify smaller-scale structures of alongshore sediment transport and partially or totally separated sedimentary cells. Some indication of their presence can be inferred from the existence of temporary divergence areas and reversals of alongshore sediment flux (Viška and Soomere, 2013b) at many locations.

In this study, we attempt to decompose the sedimentary system along a semi-isolated coast in the interior of the Gulf of Riga (Fig. 1), into partially or totally separated sedimentary cells and compartments at a resolution that matches the typical spatial scale of coastal formations in this region. As the seabed of the northern and north-eastern parts of this water body from the Sõrve Peninsula to Pärnu Bay is rocky or muddy, mostly with low availability of mobile sediment, the shoreline is heavily indented and the shallow area contains numerous islets and underwater features (Tsyrlunikov et al., 2008), we focus on the eastern, southern and western shores of the gulf that is an almost continuous sandy strip.

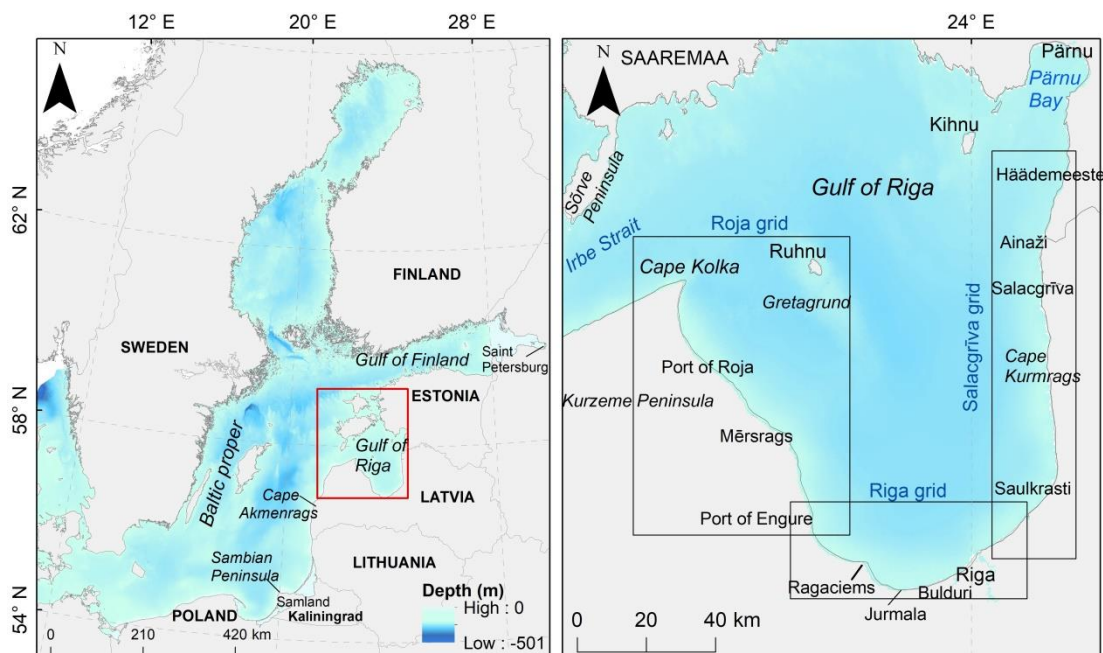


**Figure 1:** Map of the study area (left), showcasing the three subgrids of the wave model used in the analysis of wave-driven alongshore sediment transport (right). See bathymetric map of the Gulf of Riga, e.g., in Tsyrlunikov et al. (2008).



We use a set of wave time series derived from a three-level nested SWAN wave model with a spatial resolution of about 600 m. Wave-driven bulk and net potential sediment transport is evaluated using the Coastal Engineering Research Centre (CERC) approach (USACE, 2002). The results of the analysis are interpreted in terms of annual values of bulk and net potential transport. The presentation follows the classical structure of research papers. Section 2 gives an overview of study area, an insight into how the used wave data are obtained and validated, and how alongshore sediment flux is evaluated. Section 3 presents the analysis of the core properties of sediment flux in different parts of the Gulf of Riga and depicts the division of these shores into sedimentary cells and compartments. Section 4 highlights similarities and differences of sediment transport on the western, southern and eastern shores and discusses the implications of the established features for coastal processes.

## 2 Method and data

### 2.1 Study area

The Gulf of Riga (Fig. 1) is the third largest semi-enclosed subbasin of the Baltic Sea, with a surface area of 17,913 km<sup>2</sup> and an average and the maximum depth of 21 and 52 m, respectively. It has an oval-like shape with dimensions of approximately 130 × 140 km (Suursaar et al., 2002). As mentioned above, its northern and north-eastern parts have irregular bathymetry and geometry and are not addressed in this study. The bathymetry in the central part of the gulf and in the study area is regular (except for the island of Ruhnu and shallow Gretgrund to the south of this island). The width of the shallow nearshore varies insignificantly. The 10 m and 20 m isobaths are located approximately 2 km and 3.5–8 km from the shore, respectively, along the Latvian shores.

About 700,000–800,000 m<sup>3</sup> of sand is transported per year towards Cape Kolka along the north-western shore of Kurzeme Peninsula (Knaps, 1966; Viška and Soomere, 2013b) (Fig. 2). About 90 % of this mass is deposited in the vicinity of Cape Kolka and only about 50,000 m<sup>3</sup>yr<sup>-1</sup> is further transported into the sedimentary system of the Gulf of Riga (Knaps, 1966). This transport is almost entirely one-way. The accumulation area is to the north of Cape Kolka as the eastern shore of the cape is rapidly eroding (Fig. 3). The magnitude of sediment transport evaluated from observations is from 15,000 to 50,000 m<sup>3</sup>yr<sup>-1</sup> in different segments of the study area (Knaps, 1966; Ulsts, 1998). It is much smaller near Riga and remained undefined for the coastal segment to the north of Ainaži in older estimates (Knaps, 1966; Ulsts, 1998) while simulations (Viška and Soomere, 2013b) suggested that potential net transport flux continued almost unidirectionally towards Pärnu.

The observations of R. Knaps (1966) signal a complicated pattern of erosion, transit and accumulation areas in the Gulf of Riga (Fig. 2). Erosion has been observed near Roja, south of Mersrags and between Cape Kurmrags and Salacgriva while accumulation has been noted to the north of Mersrags, near Jurmala (Bulduri, Fig. 1) and Riga, and near Ainaži. These observations, stemming from the 1960s and updated in the 1990s (Ulsts, 1998), suggest that the actual pattern of sediment transport may be quite complicated.







**Figure 3:** Eroding eastern shore of Cape Kolka. Photo by T. Soomere, 2013.

140 A large alongshore variation over time in the location of the divergence area between Cape Kurmrags (Fig. 2) and  
Saulkrasti (Fig. 1) suggests that the particular location where such balance occurs may considerably vary for different years,  
giving rise to two or even more partially interconnected sedimentary cells. The analysis in this paper correlates more exactly  
the directional structure of incoming wave forcing with the bathymetry and geometry of this coastal segment and sheds more  
light on the associated structure of alongshore sediment transport in this area.

## 2.2 The SWAN model data for the nearshore of the study area

145 We employ high-resolution time series of significant wave height, average wave propagation direction and peak period  
reconstructed for the time period 1990–2022 using a triple nested version of the third-generation phase-averaged spectral  
wave model SWAN (Booij et al., 1999), developed and maintained by Delft University of Technology. The model cycle III,  
version 41.31A was forced by ERA5 wind information (Hersbach et al., 2020) in an idealised ice-free set-up. The presence  
of currents and varying water levels was ignored. A detailed overview of the particular model implementation and its  
validation for the Baltic proper and Gulf of Finland against instrumentally recorded wave data is provided in Giudici et al.  
150 (2023). An additional verification of the output of the model in the Gulf of Riga and near its entrance in the eastern Baltic  
proper as well as a thorough description of the Gulf of Riga wave climate for 1990–2021 matching the last WMO  
climatological normal (1991–2020) is provided in Najafzadeh et al. (2024).

155 This model is applied to the entire Baltic Sea at a 3 nautical mile (nmi) resolution and to the Gulf of Riga at a 1 nmi  
resolution ( $0.03^\circ$  in the East-West direction and  $0.015^\circ$  in the North-South direction). The eastern, southern and western  
coastal areas of the gulf, with a mostly straight shoreline, are covered with three realisations of a regular rectangular grid  
with a resolution of 0.32 nmi (about 600 m) (Fig. 1). The northern nearshore of the gulf (not addressed in this study) is

covered with a similar grid with a resolution of about 300 m, to adequately represent the complicated shape and irregular bathymetry in this region (Najafzadeh et al., 2024). Accordingly, the shoreline of the study area is divided into about 600–800 m long sectors depending on the mutual orientation of the shoreline and gridlines.

160 The instantaneous rate of wave-driven potential alongshore sediment transport is evaluated using the classic Coastal Engineering Research Council (CERC) approach (USACE, 2002). This model relates sediment transport in the nearshore, from the breaker line to the shoreline, with the rate of arriving wave energy flux at the breaker line, water and sediment density, and sediment porosity under the assumption of unlimited availability of sediment.

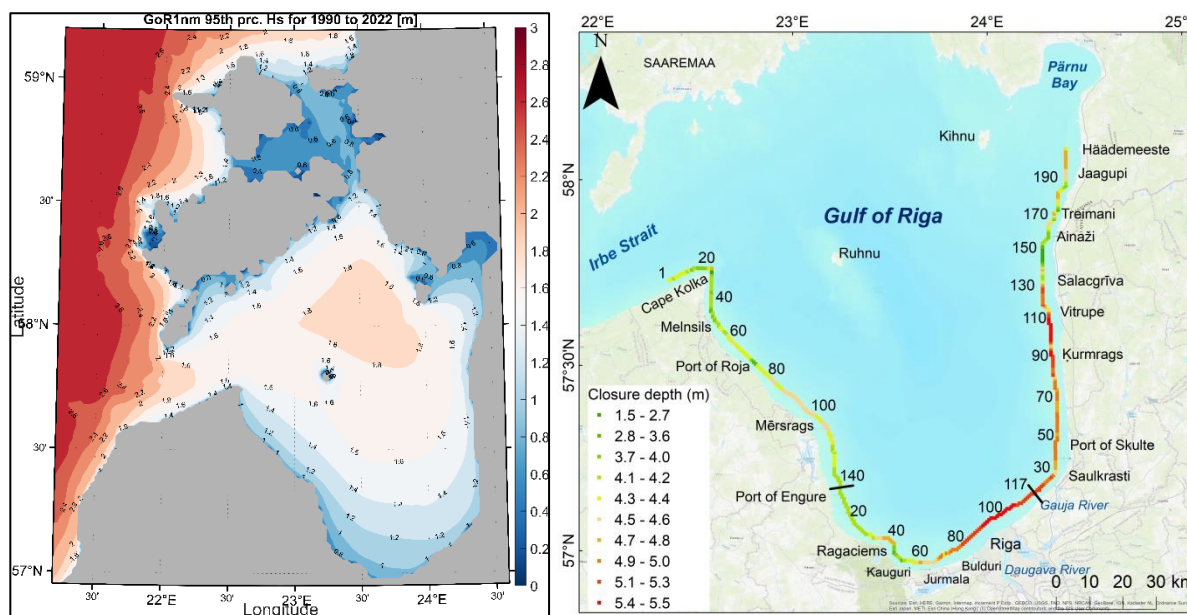
165 An adequate application of this approach thus presumes that wave properties are known somewhere offshore from the breaker line. This is a challenge for high-resolution wave models that extend almost to the shoreline. Several grid points of the wave model close to the shore have a water depth of only 1–2 m. Small waves that are adequately described by the model at such depths may serve as an important constituent of the sediment transport system in this area (Eelsalu et al., 2022). However, most sediment motion is usually generated by a few of the strongest storms in the year (Różyński, 2023). The wave climate of the eastern Baltic Sea is extremely intermittent: some 30 % of the annual wave energy flux arrives within a  
170 few days with very severe waves (Soomere and Eelsalu, 2014). Wave properties for the evaluation of wave-driven transport using the CERC model should be taken from those model grid cells that adequately reflect the most severe wave conditions. Such grid cells are normally located offshore of the breaker line.

A natural limit for water depth at which the breaker line is located is the closure depth, down to which strong waves systematically relocate sediment. The closure depth, evaluated using wave data with 5.5 km resolution data for 1970–2007,  
175 varies between 3 and 5 m (Soomere et al., 2017), being the largest near Pärnu and in the Irbe Strait. This resolution obviously does not resolve many important features of nearshore bathymetry and shore geometry in the study area.

To more adequately represent the properties of severe wave storms for the CERC model, we selected wave model grid cells for calculations of wave-driven sediment transport based on the 95<sup>th</sup> percentile wave heights, correlated with bathymetry data for proximity to estimated beach closure depths (Fig. 4). More specifically, we employed a four-step  
180 procedure for this selection. Firstly, we identified the closest cells along the shoreline that had water depth at least twice the 95th percentile of simulated significant wave height for each coastal segment. Secondly, we re-evaluated closure depth for these cells (see Soomere et al. (2017) for the description of the method and for references to the original sources). Wave simulations with a resolution of ~600 m for 1990–2022 used in this paper add several nuances to this pattern, highlighting the severity of waves in the south of the gulf near Riga and also showing that closure depth at this resolution does not  
185 necessarily follow this measure estimated using a lower resolution. As the SWAN model adequately resolves the loss and redistribution of wave energy in relatively shallow water, the closure depth estimated at this resolution may considerably depend on the water depth in a particular grid cell. For this reason, closure depth was re-evaluated for the selected cells. Based on this estimate, the selected cell was replaced by the one closer to or more remote from the coast, having in mind that the water depth in the selected cell should generally slightly exceed the closure depth evaluated for each particular location.



190 Finally, this selection was on some occasions adjusted to mirror the overall coastline shape with the set of selected grid cells and, where applicable, to maintain a more or less constant distance from the coastline.



195 **Figure 4:** Left: 95<sup>th</sup> percentile of significant wave height in the Gulf of Riga based on the SWAN model simulations 1990–2022. Right: Closure depth (color code) at wave model grid points and sequential numbers of grid cells selected for the study from three model grids (Roja, Riga and Salacgriva grids, Fig. 1) based on wave data from Giudici et al. (2023) and Najafzadeh et al. (2024). Black lines on the right panel: separation of the model grids.

The set of selected wave model grid cells contains 159 cells along the western shore of the Gulf of Riga (Roja grid, Fig. 1), 117 cells along the southern shore (Riga grid) and 201 cells along the eastern shore (Salacgriva grid). Each such cell was associated with the average orientation of the coastline and isobaths down to the closure depth. In essence, the coastline of the study area was approximated with a piecewise straight line consisting of lines with this orientation (Fig. 5). The length of such pieces varies between 560–800 m depending on the orientation of the coastline with respect to coordinate lines. Some cells were in the overlapping parts of the grids. The natural boundaries of grids were at the Port of Engure and at the Gauja River mouth. These locations are major obstacles for wave-driven alongshore sediment transport. The analysis below includes 22 cells and associated coastal sectors to the west of Cape Kolka (to provide an indication of transport along the Baltic proper shore) and 123 cells from Cape Kolka to the Port of Engure in the Roja grid, 110 cells from the Port of Engure to the Gauja River mouth along the southern shore of the Gulf of Riga, and 190 cells from the Gauja River mouth to the Estonian township of Häädemeeste along the eastern shore of the gulf.

### 2.3 Wave properties at the breaker line

210 In situations where waves usually approach the shore at a small angle between the wave propagation direction and shore normal it is reasonable to evaluate changes in wave properties from the selected wave model grid cells to the breaker line by





means of evaluation of wave shoaling and loss of wave energy due to whitewater and wave-bottom interaction using simplified formula (e.g., Larson et al., 2010). The situation is more complicated in the Baltic Sea where waves often approach the shore at large angles (Eelsalu et al., 2024a). Waves in the Gulf of Riga are usually shorter than in the Baltic proper (Eelsalu et al., 2014; Najafzadeh et al., 2024). This feature together with the narrowness of the relatively shallow nearshore (see above) implies that the impact of refraction on wave propagation is usually comparatively small and wave fields frequently approach the breaker line in the Gulf of Riga at a relatively large angle.

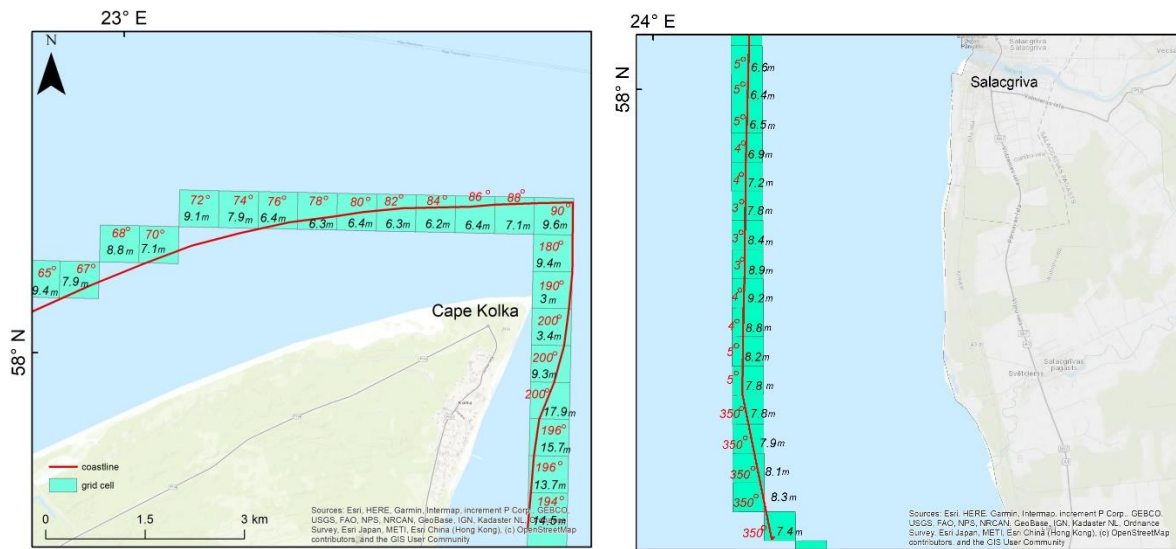


**Figure 5:** Examples of wave model grid cells used in the analysis, water depth in these cells and the associated orientation of the coastline (bold red line) near Cape Kolka (left) and Salacgriva (right).

In this case it is necessary to evaluate the joint impact of shoaling and refraction to wave properties along the path of the waves from the model grid cell to the breaker line. This can be done, to a first approximation, by assuming that the seabed decreases in depth smoothly shoreward from the wave model grid cell to the breaker line, with isobaths parallel to the shoreline. This assumption, even though not perfect, makes it possible to evaluate the joint effect of shoaling and refraction on the properties of the waves that approach the shore at a relatively large angle, during their propagation from the nearshore model grid cells to the breaker line. In the idealised case of a monochromatic wave field with a height  $H_0$  that propagates towards the shore with a phase and group speed  $c_{f0}$  and  $c_{g0}$ , respectively, and at an angle  $\theta_0$  between the wave vector and shore normal, an application of linear wave theory leads to the following algebraic equation of 6th degree for the wave height  $H_b$  at the breaker line (Soomere et al., 2013; Soomere and Viška, 2014):

$$H_b^5 g \left( 1 - \frac{H_b g \sin^2 \theta_0}{\gamma_b c_{f0}^2} \right) = H_0^4 \gamma_b c_{g0}^2 (1 - \sin^2 \theta_0). \quad (1)$$

The subscript “b” denotes the wave properties at the breaker line. A simple way to close Eq. (1) is to assume that (a) the breaking index  $\gamma_b = H_b/d_b = 0.8$  is constant (where  $d_b$  is the water depth at the breaker line) and (b) breaking waves are



long waves, which means that  $c_{gb} = c_{fb} = \sqrt{gd_b}$  at the breaker line. These approximations are not perfect: the breaking index may substantially vary (Lentz and Raubenheimer, 1999; Power et al., 2010; Raubenheimer et al., 1996, 2001; Sallenger and Holman, 1985) and breaking waves are often not ideal long waves. An advantage of these assumptions is that they make it possible, to first approximation, to systematically take into account specific features of wave fields that approach the shore at a large angle. The smaller of the two real solutions of Eq. (1) indicates the breaking wave height. The angle between the wave propagation direction and shore normal at breaking is evaluated using Snell's law.

## 2.4 Evaluation and interpretation of sediment transport

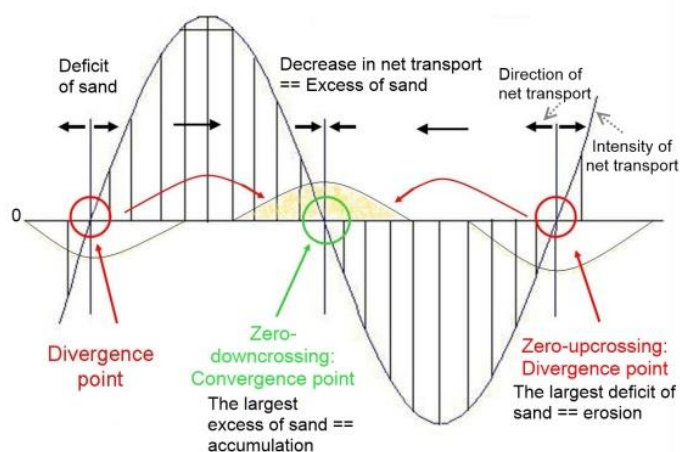
The hourly values of instantaneous potential sediment transport is evaluated for each coastal sector associated with the relevant selected wave model grid cell using the CERC approach (USACE, 2002) based on hourly time series of wave properties at the breaker line. The core approximation in the CERC formula  $I_t = KP_t = KEc_{gb} \sin \theta_b \cos \theta_b$  is that the wave-driven transport rate is proportional to the rate of beaching of the wave energy flux  $Ec_g$  ( $E$  is the wave energy at the breaker line) in the given coastal sector. The quantity  $I_t = (\rho_s - \rho)(1 - p)Q_t$  has the meaning of the potential immersed weight transport rate that is proportional to the potential alongshore sediment transport rate  $Q_t$  (USACE, 2002). The transport was interpreted as positive (counter-clockwise drift) if it was directed to the right with respect to the observer looking to the sea. The net transport for a coastal sector and a specific time period was evaluated as the sum of directional values of hourly transport, that is, taking into account the sign of  $Q_t$ . This quantity mirrors the amount of sand that would be actually transported along the shore during a certain time interval in ideal conditions. The bulk transport was calculated as the sum of absolute values of  $Q_t$ . This quantity provides an estimate of the total amount of sand that was moved in the sector in any direction, including 'back-and-forth', transport in ideal conditions.

We use constant values of porosity coefficient  $p = 0.4$  and water density  $\rho = 1004 \text{ kg m}^{-3}$  that roughly correspond to the typical material of sand (quartz) and the average salinity of  $4.90\text{--}5.38 \text{ g kg}^{-1}$  of the upper mixed layer of the Gulf of Riga (Skudra and Lips, 2017). We employ the direction-depending expression  $K = 0.05 + 2.6 \sin^2 2\theta_b + 0.007u_{mb}/w_f$  for the CERC coefficient  $K$  (USACE, 2002). Here  $u_{mb} = (H_b/2)\sqrt{g/d_b}$  is the maximum orbital velocity in linear waves,  $w_f = 1.6\sqrt{gd_{50}(\rho_s - \rho)/\rho}$  is the fall velocity. We assume that the typical grain size  $d_{50} = 0.17 \text{ mm}$  is constant and apply the density of sand  $\rho_s = 2650 \text{ kg m}^{-3}$ .

While the modelled wave time series were carefully validated against several sets of recorded wave properties (Giudici et al., 2023; Najafzadeh et al., 2024), similar validation of evaluated transport rates against direct observations of transport was not possible because of the absence of contemporary field data. For this reason, the validation was performed implicitly, by means of comparison of the results with earlier observations (Knaps, 1966; Ulsts, 1998), the output of lower-resolution simulations (Soomere and Viška, 2014), and otherwise known areas of erosion or accretion. However, as the simulated potential transport reflects the wave impact on coastal sediment in ideal conditions of unlimited availability, actual transport is usually much less intense.



265 The most interesting coastal segments are the locations of the zero-crossings of net transport. The upcrossings in this projection (positive transport direction to the right with respect to the observer looking to the sea) indicate divergence points of sediment flux and thus serve as most likely erosion areas (Fig. 6) and natural barriers separating sediment cells. The downcrossings are convergence points of sediment flux and usually mirror accumulation regions. In a similar manner, an increase in alongshore net transport from the left to the right usually reflects locations with sediment deficit and a decrease in this transport in this direction reflects accumulation regions (Fig. 6).



270

**Figure 6:** A schematic of interpretation of alongshore changes in the intensity and direction of wave-driven alongshore net transport areas (Soomere and Viška, 2014). Reprinted with permission from Elsevier, Licence 5850280172485.

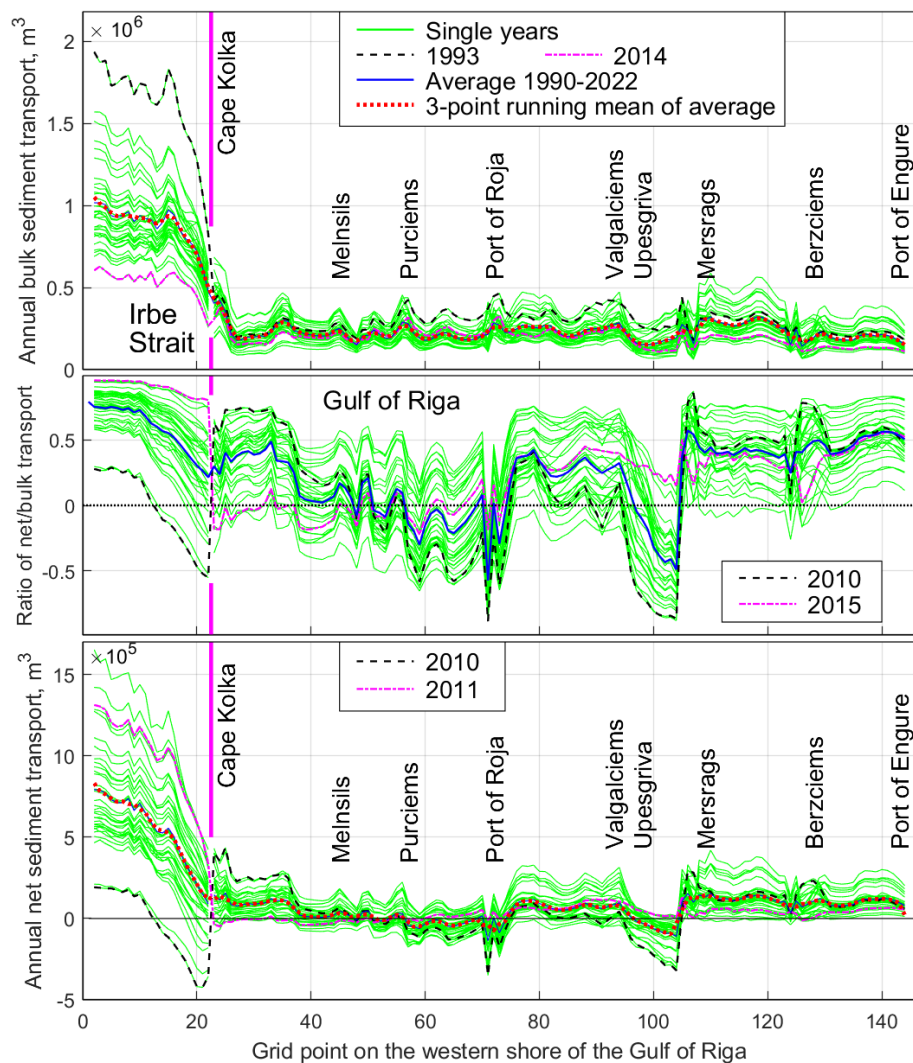
### 3 Alongshore sediment transport patterns

#### 3.1 Almost unidirectional transport along the western shore

275 We start the analysis from the western shore of the Gulf of Riga. An extension of the study area to the north-western shore of Cape Kolka provides an option to compare the results with in situ observations and earlier simulations. As expected, the intensity of potential wave-driven bulk (independent of direction) sediment transport in the interior of the Gulf of Riga is several times smaller than along the Baltic proper shore of Latvia (Fig. 7). While the typical bulk transport is about  $1,000,000 \text{ m}^3\text{yr}^{-1}$  to the west of Cape Kolka, it drops to the level of  $200,000 \pm 100,000 \text{ m}^3\text{yr}^{-1}$  to the east of the cape, with  
280 only one short segment of transport of  $300,000 \pm 200,000 \text{ m}^3\text{yr}^{-1}$  level around a headland near Mersrags. This level is also characteristic to the southern shore of the gulf as will be discussed below.

The sediment transport direction is predominantly counter-clockwise (Fig. 7, middle panel), that is, to the southeast along the western shore of the gulf. Different from many locations on the Baltic proper shores (Viška and Soomere, 2013b; Eelsalu et al., 2024a) or in the vicinity of Tallinn Bay on the northern shore of Estonia (Eelsalu et al., 2023), transport in the opposite  
285 (clockwise) direction has a considerable role between Purciems (Fig. 4) and the Port of Roja, and also between Upesgriva

and Mersrags, and in some years on the eastern shore of Cape Kolka (Fig. 7, lower panel). The latter feature is consistent with historic in situ observations (Knaps, 1966; Ulsts, 1998). The former features are not indicated in historic observations. All three reversals evidently have been smoothed out in earlier lower-resolution simulations (Viška and Soomere, 2013b) where the selected wave model grid cells lie on a straight line in this coastal segment.



290

**Figure 7:** Simulated wave-driven potential bulk sediment transport (upper panel), ratio of net to bulk transport (middle panel) and net potential sediment transport (lower panel) along the western shore of the Gulf of Riga. The blue line (average transport in 1990–2022) is almost wholly masked by the red line (3-yr running mean of the average transport in 1990–2022) in the upper and lower panels. See locations in Fig. 4.

295

While the shoreline between the eastern side of Cape Kolka and Roja is locally almost straight and gently curving, the water depth in the nearshore of this shoreline contains extensive alongshore variations in the location of selected wave model grid cells. The most significant feature is an up to 40 m deep area a few kilometres to the east of Cape Kolka (see, e.g., a



digital terrain map in Tsyrlunikov et al., 2008). This deep area becomes evident as a water depth 14–18 m in several selected wave model grid cells located less than 1 km from the shoreline (Fig. 4). The 5 m and 10 m isolines meander noticeably  
300 between Cape Kolka and Roja. This bottom structure apparently reflects streamlined topographical features in the area stemming from Late Weichselian glacial dynamics (Tsyrlunikov et al., 2008) and possibly a different orientation of ice-shaped features at a large angle with respect to the contemporary shoreline in this region during certain stages of the presence of the Fennoscandian ice-sheet (Karpin et al., 2023). This leads to considerable variations in the water depth in grid cells selected for the analysis at a scale of 1–2 km. These dissimilarities translate into local differences in the transport rates and the ratio  
305 of net and bulk transport (Fig. 7) because of reasons explained in Sect. 2.2. However, the properties of net transport are less affected and the “impact” of the described feature is almost lost in terms of averages over three adjacent grid points.

Sharp variations in the ratio of net and bulk transport near Roja reflect the presence of a small port and its wavebreakers. A discontinuity in the ratio to the west of Mersrags mirrors the presence of a headland with abruptly changing orientation of the shoreline. Still, it is likely that, at least in some years, the overall counter-clockwise sediment transport carries sand  
310 around this headland to the south-east. The breakwaters of Port of Engure extend further from the shoreline than those of Port of Roja and Port of Mersrags and apparently discontinue this transport.

The pattern of the magnitude of annual net sediment transport reinforces and provides detail to these conjectures. The typical rate of counter-clockwise net transport on the Baltic proper shore of Cape Kolka varies from 300,000 to 900,000  $\text{m}^3\text{yr}^{-1}$ , depending on the particular coastal section, with an average of about 600,000  $\text{m}^3\text{yr}^{-1}$  over a 10 km long stretch to the  
315 west of the cape (Fig. 7). This projection matches the outcome of earlier in situ observations (Knaps, 1966; Ulsts, 1998) and simulations (Soomere and Viška, 2014).

The properties of bulk and net transport vary significantly in different years. The years characterised by very intense (e.g., 1993) or very low (e.g., 2014) bulk transport along the northwestern shore of Cape Kolka are not mirrored along the coastal stretch to the east of Cape Kolka. The same feature is evident for the ratio of net and bulk transport (years 2010 and  
320 2015 in the middle panel of Fig. 7) and for the net transport. The characteristic feature of the net transport is that years with strong counter-clockwise transport to the west of Cape Kolka (e.g., 2011) correspond to almost zero counter-clockwise transport in the western Gulf of Riga. The change in the sign of the net transport at Cape Kolka in years with strong clockwise transport to the east of the cape (e.g., 2010) evidently reflects the role of northerly winds in such years. These winds drive sand transport to the south near the cape. This transport is negative (clockwise) to the west of the cape and  
325 positive (counter-clockwise) to the east of the cape. The major jump in most of the annual values of the net transport and the ratio of net and bulk transport at Cape Kolka is highlighted using the values of this transport in two single years, in Fig. 7. Interestingly, there is no jump or discontinuity in the average net transport or the ratio of net and bulk transport at this location. Another interesting feature is that the ratio of the net and bulk transport may considerably vary with respect to the average value of this ratio in single years (e.g., 2010 and 2015 in Fig. 7).

330 The intensity of potential net transport varies considerably along the western shore of the Gulf of Riga. Its average magnitude from Cape Kolka to Engure is about 50,000  $\text{m}^3\text{yr}^{-1}$ , and this is consistent with previous findings. The presence of





a zero-downcrossing of net transport in some years immediately to the east of Cape Kolka (around cell #25) mirrors the presence of an erosion area in this location (Fig. 3). Even though there are several locations of relatively frequently occurring pairs of zero-downcrossings between Cape Kolka and the headland near Mersrags, this coastal segment most likely forms a continuous sedimentary system in which sand can move along the entire segment in different years. The shoreline of this area is slightly curved and several sand bars exist in the nearshore along the entire section. Small-scale fluctuations in the numerically evaluated bulk sediment transport and reversals of net transport between Cape Kolka and Roja apparently stem from the choice of particular locations of selected wave model grid cells.

It is likely that breakwaters of the Port of Roja largely stop alongshore sediment flux. Technically, this feature is reflected by a local reversal of net sediment transport in the coastal sector corresponding to wave model grid cell #71. Relatively intense net sediment transport evidently takes place between Roja and a headland to the west of Mersrags. The impact of a few small-scale headlands and jetties at grid cells #74 and #79 interrupts the continuous sand beach and partially stops sediment transport. Their impact is not resolved by the model.

A major headland to the north of Mersrags almost completely stops the counter-clockwise transport. The orientation of the coastline changes by about 80 degrees. This feature is visible in Fig. 7 as a reversal of net sediment transport in most years. It is therefore safe to say that even in the absence of harbours and breakwaters the coastal segment from Cape Kolka to the headland at Mersrags formed an almost isolated sedimentary compartment in the past that was to some extent fed by sand from the vicinity of Cape Kolka.

A direct consequence is that there is almost no sand on the eastern side of this headland and also in the vicinity of the Port of Mersrags. Additionally, the Port of Mersrags almost fully stops sediment transport even though this feature is not resolved in our simulations. The sandy beach becomes evident again about 10 km to the south of Mersrags.

Similar to the described pattern, the coastal stretch between Mersrags and Engure contains a few minor headlands that to some extent modulate the intensity of both bulk and net transport, and their ratio. Different from the above, this stretch contains almost entirely (in terms of annual means) counter-clockwise sediment transport. Reversals occur only in a couple of years. Breakwaters of the Port of Engure (not shown in Fig. 7) and accretional features at these breakwaters almost fully stop the wave-driven sediment transport. Together with the headland at Mersrags they separate this coastal stretch into an almost isolated sedimentary compartment.

### **3.2 Variable transport and accumulation along the southern shore**

The southern coast of the Gulf of Riga changes its orientation from North-South direction at Engure (Fig. 4), to West-East direction near Jūrmala and to Southwest-Northeast near the Gauja River mouth (Fig. 1). This pattern of changes means that the largest driver of sediment transport between Engure and Jūrmala are waves generated by northerly winds while the predominant driver near Riga (Daugava River mouth) and further to the east are south-westerly winds, the fetch length of which increases from the west to the east. The coastline is smoothly curved from Engure to Ragaciems (Fig. 4), with a gentle headland at Ragaciems, and is again gently curved from Ragaciems to the Daugava River mouth and to the north-east of the



365 Daugava River mouth. The massive breakwaters at the river mouth (Fig. 8) almost completely stop wave-driven alongshore transport and divide the coastal stretch into two almost totally separated sedimentary compartments.

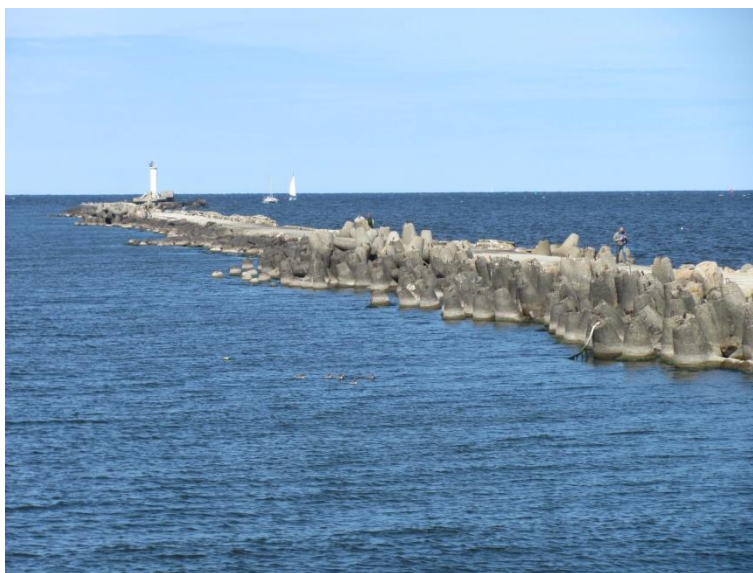


**Figure 8:** Western breakwater at the Daugava River mouth. Photo by T. Soomere, 2019.

The local variations in transport are much larger than on the western shore of the Gulf of Riga. The situation between the  
370 Port of Engure and Kesterciems (Fig. 9) resembles the situation between Mersrags and Engure (Fig. 7). Both coastal segments contain a few minor headlands that to some extent modulate the intensity of both bulk and net transport, and their ratio. As the orientation of the coastline changes more to the east at Kesterciems, it is natural that bulk sediment transport slows to the level of  $50,000 \text{ m}^3\text{yr}^{-1}$  on the section between Kesterciems and Ragaciems where waves from the north approach the shore at a gradually larger angle. This transport increases again at Ragaciems where both predominant wave  
375 systems result in transport in the same direction. It slows down in the vicinity of Jūrmala where northerly waves approach the shore at a small angle and provide only a small contribution to the transport, and waves created by south-western winds are weak. The scale of calculations resolves the impact of a small headland at Kauguri (Fig. 4) and the presence of depositional features on both sides of jetties of the Daugava River mouth. The typical bulk sediment transport is from  $50,000 \text{ m}^3\text{yr}^{-1}$  in gently curved coastal segments to  $300,000 \text{ m}^3\text{yr}^{-1}$  near headlands. It is much larger on both sides of the Daugava  
380 River mouth and is relatively intense (about  $150,000 \text{ m}^3\text{yr}^{-1}$ ) to the north-east of the Daugava River mouth.

The long-term average transport is predominantly to the south-east and east in the western part of this area. The transport is almost unidirectional (counter-clockwise) in coastal segments to the south of Engure, to the south-east of Ragaciems and in most of the area between mouths of Daugava River and Gauja River (Fig. 9). It is also almost unidirectional along the coast of Jūrmala. The transport direction varies considerably in single years in the area to the north of Ragaciems. A clear  
385 reversal is present near the Daugava River mouth because of a large depositional feature in this area that modifies the orientation of the coastline.

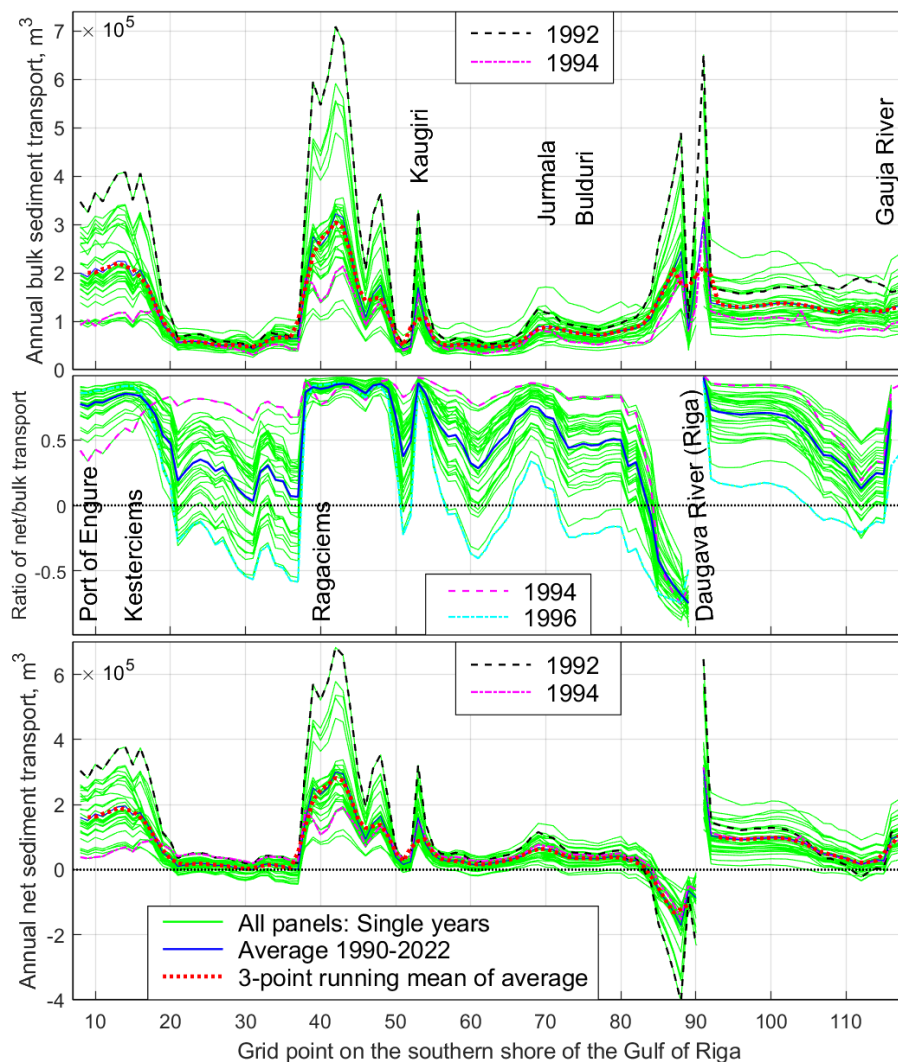


**Figure 9:** Simulated wave-driven potential bulk potential sediment transport (upper panel), ratio of net transport (middle panel) and net transport (lower panel) along the southern shore of the Gulf of Riga from the Port of Engure to the Gauja River mouth. Note different vertical scales of the upper and lower panels compared to Fig 7. The data for grid points that follow the orientation of breakwaters of the Port of Engure and jetties at the Daugava River mouth are omitted. See locations in Fig. 4.

The average annual net transport is much smaller in this segment, well below  $50,000 \text{ m}^3\text{yr}^{-1}$ , with an exception near Engure and around Ragaciems where the simulated average values are almost  $200,000 \text{ m}^3\text{yr}^{-1}$  and up to  $600,000 \text{ m}^3\text{yr}^{-1}$  in single years in a small segment. These estimates match well the historical in situ estimates; however, earlier simulations (Viška and Soomere, 2013b) suggest much more powerful alongshore sediment flux in the vicinity of the Daugava River mouth. Consistent with the above-discussed features, alongshore net transport is almost zero along the gently curved coastal stretch from Kesterciems to Ragaciems and in the vicinity of Jūrmala. The alongshore variations in transport indicate that the vicinity of Klapkalnciems and Jūrmala are sediment accumulation areas. A clear reversal of sediment transport at the



400 Daugava River mouth most probably represents the impact of long-term riverine sediment transport into this area and signals that wave impact works against the formation of a river delta.

Different from the situation on the western coast of the gulf, sediment transport is high along the entire coastal stretch in years of intense transport (e.g., 1992) and low along the entire stretch in years of less intense transport (e.g., 1994). The years with intense bulk transport have also strong net transport (e.g., 1992) and vice versa (e.g., 1994). In a similar manner, years with predominantly unidirectional transport have this property along the entire coastal segment (e.g., 1996), except in the immediate vicinity of the western breakwater of the Daugava River mouth while in years with frequent reversals of this transport reversals occur in about half of this segment. This structure of net transport suggests that the segment in question contains three sedimentary compartments, separated by the headland at Ragaciems and breakwaters of the Daugava River mouth. While sediment from the easternmost system can be transported across the headland at Ragaciems, reverse transport is highly unlikely at an annual scale. The compartment from Kauguri to the western breakwater of the Daugava River mouth may be considered as a combination of two cells with almost unidirectional sediment exchange between them.

### 3.3 Fragmented eastern shore

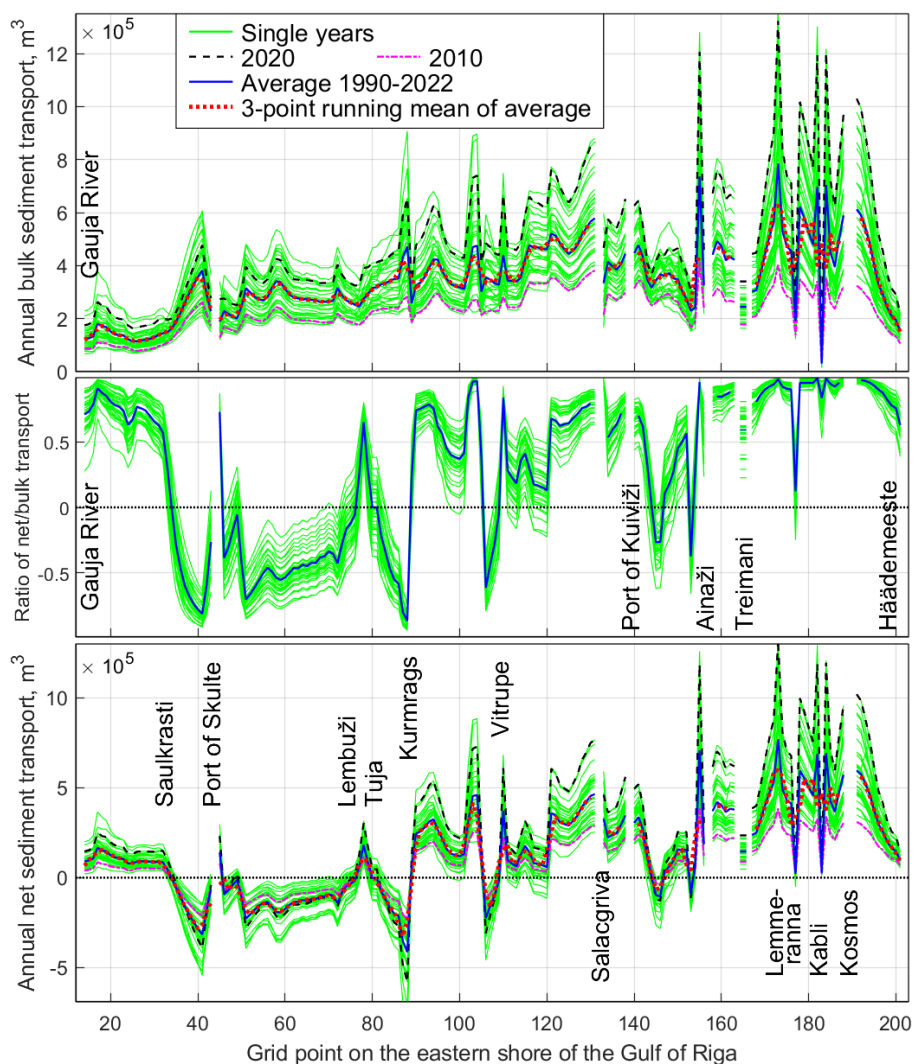
The eastern shore of the Gulf of Riga (Fig. 1, 2) from the Gauja River mouth to the Estonian township Häädemeste (Fig. 4), even though generally almost straight, contains one larger (Cape Kurmrags) and several smaller variations in the coastline orientation. Historical in situ observations (Knaps, 1966; Ulsts, 1998) suggest that this area may have several erosion and accumulation areas (Fig. 2) and possibly also several sedimentary cells that are more or less isolated from each other in terms of annual sediment transport.

Different from the western and southern shores of the Gulf of Riga, the sandy shore is not continuous in this area. Some coastal segments have cobble and boulder pavement, and consist of material that is not easily erodible, or are rocky (e.g., at Kuiviži). Several coastal segments in the vicinity of the Latvian-Estonian border and Häädemeste are almost completely devoid of sand and wave driven sediment transport is very limited. Therefore, the actual transport, evaluated in Knaps (1966) and Ulsts (1998), may well be just a small fraction of the simulated potential transport.

This coastal segment is evolving, similar to the Latvian and Lithuanian Baltic proper shores, under a delicate balance of two predominant wave systems (Eelsalu et al., 2024b) that in this case work exactly against each other. This is the natural reason why the potential bulk transport (Fig. 10) increases from about  $150,000 \text{ m}^3 \text{ yr}^{-1}$  in the south to about  $400,000 \text{ m}^3 \text{ yr}^{-1}$  in the north: while the properties of waves generated by the north-north-western winds do not change much, the impact of waves excited by south-western winds increases with the increase of fetch length for these winds.

The transport direction along this stretch is highly variable (Fig. 10), with typical lengths of unidirectional transport of only a few kilometres. The transport in the region immediately to the east of the Gauja River mouth is almost fully counter-clockwise to the northeast. The transport is predominantly clockwise from Saulkrasti to Cape Kurmrags, has a variable direction from Cape Kurmrags to Ainaži at the Latvian-Estonian border, and is predominantly to the north (counter-clockwise) in the Estonian part of the study area. This variation apparently mimics changes in the orientation of the shoreline

and the changing balance of the fetch lengths of southerly and northerly winds. These lengths are more or less equal in the middle of this coastal stretch. The nearshore of its northern part is to some extent sheltered against waves from the north, north-northwest and north-west by the island of Kihnu and the Estonian mainland.



435

**Figure 10:** Simulated wave-driven potential bulk potential sediment transport (upper panel), ratio of net transport (middle panel) and net transport (lower panel) along the eastern shore of the Gulf of Riga. Note different vertical scales of the upper and lower panels compared to Figs. 7 and 9. The data for grid points that follow the orientation of breakwaters of the Port of Skulte, Salacgrīva, Kuivīži, Treimani and at Kosmos are omitted. See locations in Fig. 4.

440

Consistent with Viška and Soomere (2013b), the average potential net transport along this stretch varies considerably, between about 15,000 and 590,000  $\text{m}^3\text{yr}^{-1}$  (in terms of 3-point running average, Fig. 10). Its intensity generally increases from the south to the north similar to the bulk transport. There are several persistent zero-upcrossings in the net sediment transport, together with alongshore variations of the ratio of net and bulk transport (Fig. 10). These features signal that the





445 sedimentary system of the eastern coast of the Gulf of Riga is highly fragmented. This feature was not resolved by earlier simulations (Viška and Soomere, 2013b; Soomere and Viška, 2014) that provided a highly generalised picture of the system. Consequently, long-range transport of sediment along this coastal section is unlikely and there are several natural reversals of the overall counter-clockwise sediment transport pattern along with associated sediment erosion and accumulation regions.

450 The presence of several man-made structures, such as the Port of Skulte, jetties at Salacgriva, Kuivīži, Ainaži, Treimani and the historical recreation centre for USSR astronauts (Kosmos in Fig. 10) augments the fragmentation. Together with headlands such as Cape Kurmrags and other smaller headlands that serve as invisible barriers to sediment transport, they separate the coastal stretch into numerous almost isolated sedimentary cells with a typical length of 5–25 km. The longest interconnected coastal segments are near Saulkrasti (ca 21 km), from the Port of Skulte to Cape Kurmrags (ca 25 km), from Vitrupe to Salacgriva (ca 16 km), and from Treimani to Kosmos (ca 14 km).

455 The breakwaters of the Port of Skulte are apparently a major obstacle to sediment transport and delineate the northern end of the sedimentary compartment between the port and the Gauja River mouth. The region to the south-west of these jetties apparently is an accumulation area and the area to the north is likely subject to erosion. The accumulation feature at the Gauja River mouth and the associated change in the orientation of the coastline give rise to a local net sediment transport reversal in single years but still allows counter-clockwise sediment flow to the north in most years. A clear sediment flux convergence area at Saulkrasti (Fig. 10) matches the presence of a long and wide sandy beach. Together with an extensive sediment transport reversal that apparently extends to Lembuži and possibly even to Kurmrags, its presence signals that the Saulkrasti region has been the end location of counter-clockwise sand motion along the rest of the Gulf of Riga shores. This conjecture is supported by the absence of any notable accumulation feature adjacent to the southern breakwater of the Port of Skulte about 6 km to the north of Saulkrasti.

465 Figure 10 indicates the presence of a persistent reversal area of net sediment transport to the north of Saulkrasti. This reversal signals that waves from the northern directions dominate the wave-driven transport over this more than 30 km long segment (that is split into two parts by the Port of Skulte). It is not clear whether a minor headland near Lembuži serves as a major barrier of net transport. Even though it creates a zero-upcrossing of annual net sediment transport, it is likely that wave-driven sediment flux passes this headland on many occasions and that the coastal segment from the Port of Skulte to Cape Kurmrags is a connected compartment.

475 The most significant net sediment flux divergence area is located at Cape Kurmrags, essentially a very minor headland that insignificantly extends into the sea. Together with a sister headland about three kilometres to the north, they are an almost impermeable barrier for wave-driven sediment motion in our model in terms of annual average sediment transport. As single storms still can move sediment around these capes, the sedimentary systems to the north and south of these capes are not totally isolated from each other.

While bulk transport gradually increases from the south to the north between Cape Kurmrags and Salacgriva, net transport greatly varies in this segment. It has a short but clear reversal in terms of annual values near Vitrupe. Similar to the



above, it is likely that waves in single storms carry sediment across this location and thus the coastal segment from Cape Kurmrags to Salacgriva is a connected sedimentary compartment. Extensive variations in the intensity of potential net  
480 transport indicate areas prone to erosion (if this increases from the left to the right, Fig. 6) or accumulation (segments in which the net transport accordingly decreases) in this compartment.

Sediment transport at and to the north of Salacgriva is fragmented. Several minor headlands to the south of Salacgriva modulate the transport properties but do not serve as barriers. Jetties on both sides of the Salaca River and Kuivižu River mouths almost totally block alongshore sediment transport. The same applies to jetties at Ainaži, Treimani and Kosmos. As  
485 the coast to the north of Cape Kurmrags contains very limited fine sediment, the simulated (potential) sediment transport by at least an order of magnitude exceeds the actual wave-driven transport. The nature of the coast and the location and size of accumulation features at different obstacles confirms that the transport is predominantly to the north.

The properties of transport in single years have many particular features in this coastal segment. The years with intense bulk transport generate large transport throughout the segment. In a similar manner, in years with low bulk transport the  
490 intensity of bulk transport is low over the entire segment (Fig. 10, upper panel). Interestingly, this feature is not true for the net transport. While its intensity in the northern part of the segment matches the intensity of bulk transport, the situation is different in the south, especially between the Port of Skulte and Cape Kurmrags, where net transport in these years is at the average level.

### 3.4 Potential bulk and net alongshore sediment transport over the entire area

495 Estimates of interannual and decadal variations in the bulk and wave-driven potential sediment transport integrated along the eastern Baltic Sea (Soomere et al., 2015) have revealed a major regime shift in transport properties around the year 1990. While potential bulk transport integrated from Samland to Pärnu continued to grow 1970–2007, net transport increased only until about 1990 and decreased 1990–2007. This process was primarily driven by changes that occurred on the Baltic proper shore of the Kaliningrad District (of Russia), Lithuania and Latvia. It almost did not become evident on the shores of the  
500 Gulf of Riga where bulk potential transport even decreased to some extent 1990–2007 but net transport was at an almost constant level (Viška and Soomere, 2013a).

A possible reason for the loss of this probable signal of climate change in the Gulf of Riga may be the use of values of potential transport integrated over the entire set of its western, southern and eastern shores. As these shores are oriented very differently with respect to predominant wind directions, it is likely that such a signal is present on some of these shores only.

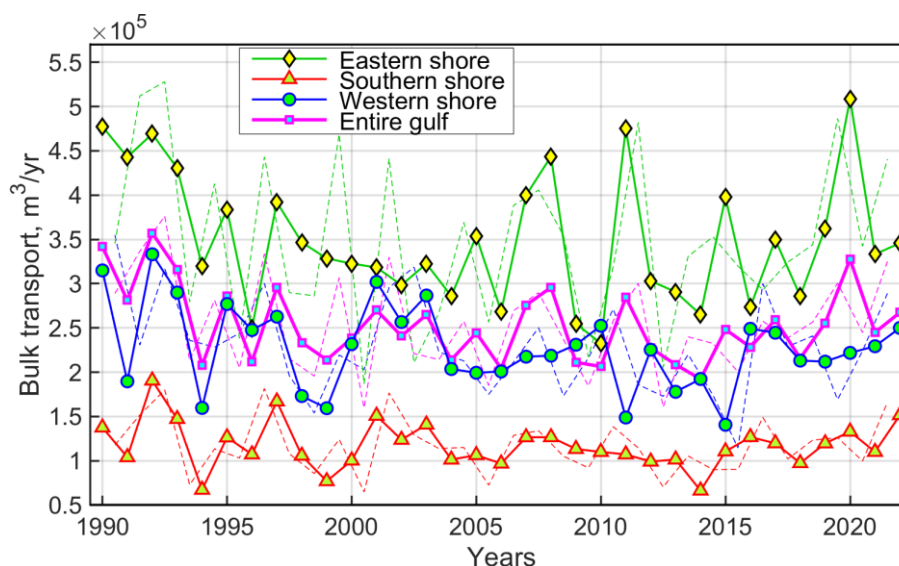
505 The average intensity of potential alongshore sediment transport per grid cell is largest on the eastern shore of the Gulf of Riga (Fig. 11). The location and orientation of this segment is such that high waves generated by predominant strong winds commonly arrive at the coast at a large angle and thus generate strong alongshore transport. This does not automatically mean massive net or actual sediment transport. Almost the entire eastern shore of the Gulf of Riga (except for accumulation area at Saulkrasti) suffers from a deficit of sediment (Knaps, 1966; Ulsts, 1998). Consequently, the magnitude of actual  
510 sediment transport along this shore is only a small fraction of the potential transport.

The potential sediment transport is considerably weaker on the other shores of the Gulf of Riga. Its magnitude on the western shore is, on average, about 50 % of that on the eastern shore and only about 30 % of that on the southern shore (Fig. 11). These differences evidently reflect the combination of the direction of predominant winds and orientation of the coastal segments. While northerly winds apparently generate the same magnitude of potential transport on the eastern and western shores, the contribution of waves driven by westerly winds is almost missing on the western shore. This explains the difference in transport of a factor of two. Similarly, waves created by westerly winds are still low on the southern shore even though they arrive at this shore segment at a large angle. Waves driven by northerly winds are commonly much stronger but they arrive at a small angle and usually do not generate massive alongshore transport.

515

The temporal course of bulk transport does not increase gradually as found by Soomere et al. (2015) for Samland to Pärnu for 1970–2007. Instead, this transport decreases by up to 30% on the eastern and western shores of the gulf 1990–2005 and exhibits no obvious trend 2005–2022. This pattern is, however, consistent with the course of bulk sediment transport integrated from Cape Kolka to Pärnu Bay (Viška and Soomere, 2013a). Interestingly, Viška and Soomere (2013a) also indicated maxima in this quantity around the years 2004 and 2007.

520



525 **Figure 11:** Average annual (solid lines with markers) and storm season (thin dashed lines) potential bulk sediment transport per wave model grid cell along western, southern and eastern shores of the Gulf of Riga 1990–2022.

530

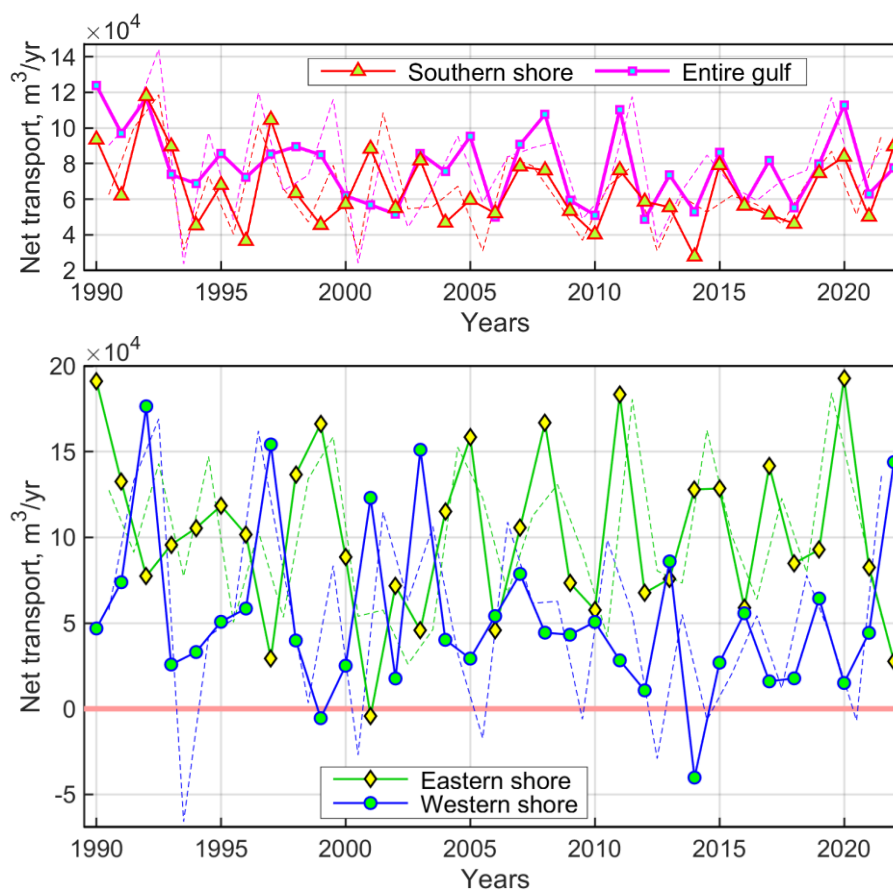
It is therefore likely that the intensity of wave-driven sediment transport and thus also coastal processes in the interior of the Gulf of Riga develop independently from, or even in counterphase, with respect to transport on the shores of eastern Baltic proper. The probable reason is the presence of long coastal segments in the gulf that are differently oriented with respect to the predominant wind directions.

Another implication of this feature becomes evident as the difference in the pattern of interannual variations of bulk transport on different shore segments. Namely, transport on the eastern and western shores of the gulf contains extensive interannual variations but with no obvious trend 2005–2022. The situation was different on the southern shore where



transport had large interannual variations 1990–2005 but has been almost steady since then. It likely that this difference  
535 reflects different temporal patterns of changes to winds from the two predominant directions that become evident in  
differently oriented segments.

Additional information about the structure of the temporal course of transport is provided by analysis of transport during  
so-called storm seasons, specifically, 12-month time periods from July to June of subsequent year (Männikus et al., 2019,  
Eelsalu et al., 2022). The use of such time periods (Fig. 11, 12) often better characterises the severity of winds in the  
540 relatively windy autumn and winter seasons, and thus also of interannual variability of sediment transport intensity. The  
differences between this quantity and annual bulk transport are relatively large on the eastern shore and fairly small on the  
southern shore. Consistent with the above, this quantity does not exhibit any significant trend since 2005. Moreover, the  
course of this quantity signals that the decrease in annual values of the bulk transport along the western shore in the 1990s  
simply reflects improper clustering of the underlying data into annual values.



545

**Figure 12:** Average annual (solid lines) and storm season (thin dashed lines) potential net sediment transport per wave model grid cell along western, southern and eastern shores of the Gulf of Riga in single years 1990–2022.

Different from above but consistent with Viška and Soomere (2013a), average potential net sediment transport integrated  
550 over the entire study area (Fig. 12) displays almost no long-term and decadal changes. It also exhibits much smaller



interannual variations than bulk transport in single segments (Fig. 10). Interannual variations in the net transport are, however, significantly different in the three coastal segments. While these variations are fairly limited on the southern shore, they exceed by an order of magnitude the average level of these quantities on the western and eastern shores. Interestingly, most of these large variations are exactly in counter-phase on the western and eastern shores. When the net transport is  
555 integrated over the two segments, these variations cancel each other and lead to limited interannual variations of the total net transport. The pattern of variations of net transport over different storm years mostly mimics the pattern for calendar years.

#### 4 Discussion and conclusions

The new high-resolution wave data from the SWAN model allowed for a vital update of the earlier estimates of wave-driven potential sediment transport rates, their interannual and decadal variations, location of divergence and convergence areas of  
560 the sediment flux and associated patterns of sedimentary compartments and cells on the sedimentary shores of the Gulf of Riga.

##### 4.1 General sediment transport patterns

The simulations reinforced the well-known predominant counter-clockwise pattern of wave-driven sediment transport along the western, southern and eastern shores of the Gulf of Riga. The main advance from the material presented here is a more  
565 detailed and substantiated pattern of transport, identification of major transit regions and divergence (erosion) and convergence (accumulation) areas on these shores. Together with locations of harbours and cells these areas define the extent and location of the major sedimentary compartments and cells (Fig. 13).

The simulations have highlighted different structural properties of sediment transport on the western, southern and eastern shores of the gulf.

570 The short coastal section immediately to the south-east of Cape Kolka has a clearly visible erosion point associated with a frequent divergence of sediment flux. The western shore from Cape Kolka to a headland to the north of Mersrags has relatively intense counter-clockwise transport that is reversed in some years. It apparently formed a large interconnected sedimentary compartment in the past that is now split into almost isolated cells by breakwaters and jetties. The shore segment to the south of Mersrags to the Port of Engure forms another interconnected sedimentary compartment.

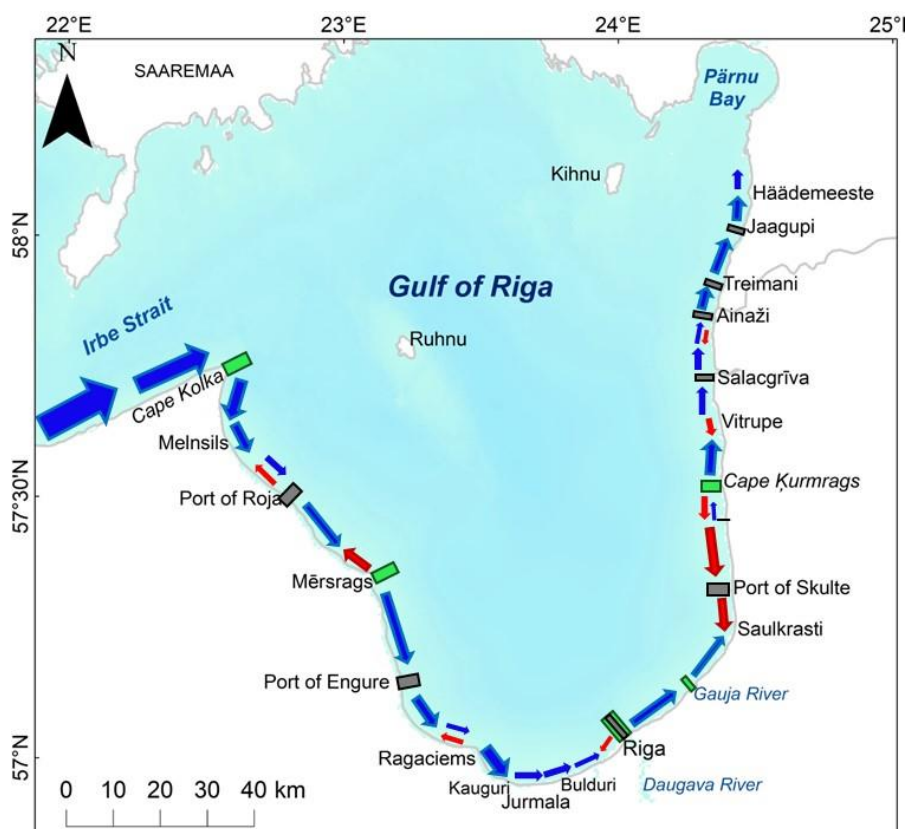
575 The southern shore has much less intense and more unidirectional counter-clockwise sediment transport that encompasses the entire segment and weakens to the east towards some extensive accumulation areas. The vicinity of the Daugava River mouth became a major end point of this transport after construction of jetties. Part of this transport may have passed the river mouth in the past and reached the ultimate end location at Saulkrasti.

580 The potential sediment transport is much larger along the eastern shore than the southern shore and increases from the south to the north. This shore contains a longer segment of predominantly clockwise transport and is split into two almost separated sedimentary compartments by an area of divergence of sediment flux near Cape Kurmrags. The compartment to





the north of Cape Kurmrag is split into several smaller almost isolated sedimentary cells by breakwaters and jetties. The deficit of fine sediment severely limits the actual transport.



585 **Figure 13:** Transport directions (arrow widths correspond to the rate of potential net transport), major interconnected sedimentary compartments separated by major natural divergence points of net sediment transport (green rectangles), and large harbours and jetties (black rectangles) that split the sedimentary compartments into almost separated cells. Blue arrows indicate counter-clockwise transport and red arrows show clockwise transport. Parallel narrow blue and red arrows denote variable transport regime in different years.

#### 4.2 Interannual and decadal variations in sediment transport

590 The simulations highlighted a mismatch of decadal variations in the wave-driven sediment transport in the interior of the Gulf of Riga (Viška and Soomere, 2013a) from those identified for longer segments of the eastern Baltic Sea proper (Viska and Soomere, 2013b). The reason is the specific orientation of some shore segments of the gulf with respect to the predominant moderate and strong winds (usually south-western, and north-north-western, Soomere, 2003) that create the majority of waves responsible for sediment transport.

595 These winds generate radically different transport properties on differently oriented western, southern and eastern shores of the gulf. The western shore is mostly affected by northerly winds. Waves generated by these winds approach the shore at a large angle with respect to the shore normal and thus, if present, drive intense counter-clockwise transport over long

distances. Winds from south-west blow to the offshore over this coastal segment and only occasionally contribute to the clockwise transport. Thus, counter-clockwise transport usually prevails and its magnitude is mostly governed by the properties of the northerly winds.

The southern shore is jointly affected by frequent but relative weak and short waves created by south-western winds and occasionally waves excited by strong but less frequent northerly winds. The latter waves usually approach the shore at a small angle and thus do not generate strong alongshore transport. As a result, the intensity of both bulk and net transport is low and accumulation predominates over long sections of the southern shore.

The eastern shore experiences strong waves generated by both south-western and northerly winds. Both wave systems can be strong and often arrive at the shore at a large angle. Therefore, the direction of transport is jointly covered by these two wave systems. The instantaneous transport direction is thus variable and the annual average reflects the balance of the wave systems in a particular year. The only exception is the southernmost part of the shore at Saulkrasti that is as an end point of transport from the west and from the north.

It is therefore natural that the balance of the two components of the local bi-directional structure of moderate and strong winds together with the different orientation of the shoreline in the three coastal segments translates into an interesting mismatch of wave-driven transport properties on the western and eastern shores of the gulf (Fig. 12).

The intensity of bulk transport combines the joint impact of both wave systems and thus largely follows variations in wind speed. The intensity of net transport additionally expresses the changing role of these wave systems. Stronger than average waves from the northerly directions result in stronger than average transport to the south on both eastern and western shores. This means more intense than usual counter-clockwise transport on the western shore and more intense than usual clockwise transport on the eastern shore.

This property naturally translates into a mirrored pattern of time periods of high and low net potential transport on the western and eastern shores of the Gulf of Riga (Fig. 12). This pattern underscores a highly interesting feature of the dynamics of the Gulf of Riga: almost regular fluctuations in the role of northerly winds in the system with almost constant amplitude and with a time scale of 3–4 years (Fig. 12).

### 4.3 Implications for coastal processes

The presented features also translate into several observations with respect to the difference of structural properties of sediment transport and connectivity in the three coastal segments. It is likely that synchronisation of water levels and wave approach (and sediment transport) directions supports the stability of relatively small beaches or sedimentary cells (Eelsalu et al., 2022). This mechanism apparently is not applicable on the western and southern shores of the gulf where large excursions of sediment parcels and long sections of transit are typical. Both these segments contain only one major divergence area that may serve as a barrier for sediment transport and only a couple of man-made structures limit the transport range. This mechanism may, however, become apparent on the eastern shore that is divided into several smaller cells by one major divergence area and several jetties or moles.



The presence of long interconnected sedimentary compartments signals that strong storms may bring large amounts of sediment into motion. A typical consequence of this feature is rapid straightening of parts of the coast, a process that has already created numerous coastal lakes near the eastern shore and turned the river mouths down-drift on the southern shore of the Gulf of Riga. Another possible consequence is siltation of harbour entrance channels. These processes are much less  
635 intense on the eastern shore in spite of the even larger intensity of wave-driven potential transport. A concealed feature is the potential large spread of hazardous materials in the event of sediment contamination along the western and southern shores.

In this context, the presented high-resolution simulations provide valuable insights into sediment transport patterns along the Gulf of Riga coastlines compared to older, essentially basic estimates from in situ observations (Knaps, 1966; Ulsts, 1998) and earlier low-resolution simulations (Soomere and Viška, 2014). These findings aid in the planning of harbour and  
640 coastal infrastructure as well in the assessment of several kinds of environmental impacts.

The decomposition of the sedimentary system of the Gulf of Riga into smaller compartments and cells provides vital information for management solutions and importantly for the identification of potential erosion and accumulation areas. This information is crucial for developing and closing the sediment budget in this microtidal water body. It also indicates how far sediment may be transported from a particular location under the current wind and wave climate. The results are  
645 largely invariant with respect to grain size and sediment availability (unless the grain size varies strongly over short distances) even if the potential transport greatly exceeds actual transport. A natural extension of this research would be a similar analysis of sediment transport, compartments and cells along the sedimentary shores of the Baltic proper, ideally including the Polish coastline.

650 *Code and data availability.* Time series of simulated wave properties in the selected wave model grid cells and information about these cells and proxy shoreline orientation are available on request from the authors (mikolaj.jankowski@taltech.ee). The software developed for this study is essentially an almost trivial counting exercise of hourly wave-driven potential transport, and is available on request from the authors.

655 *Author contribution.* TS and KEP designed the study, created interpretation of the outcome, and prepared the manuscript with contributions from all other co-authors. TS performed analysis of spatial and interannual variations in the transport. MZJ carried out the analysis of wave data, selection of wave model grid cells and calculations of transport properties, and wrote the relevant sections of the manuscript. ME developed the proxy coastline, validated the outcome and created geographical visualisation. MV contributed geographical and geological data of the study area and linked this information  
660 with the outcome of simulations. In the CRediT contributor roles taxonomy: TS: Writing – original draft, review & editing, Visualization, Validation, Software, Methodology, Formal analysis, Supervision, Funding acquisition, Project administration. MZJ: Writing – single parts, Software, Investigation, Validation, Formal analysis, Visualization. ME & MV: Investigation, Validation, Visualization. KEP: Supervision, Methodology, Writing – review & editing.



665 *Competing interests.* The authors declare that they have no competing interests.

*Acknowledgements.* The research was co-supported by the Estonian Research Council (grant PRG1129) and the European Economic Area (EEA) Financial Mechanism 2014–2021 Baltic Research Programme (grant EMP480).

## References

- 670 Aagaard, T., Brinkkemper, J., Christensen, D. F., Hughes, M. G., and Ruessink, G.: Surf zone turbulence and suspended sediment dynamics—A review, *J. Mar. Sci. Eng.*, 9, 1300, <https://doi.org/10.3390/jmse9111300>, 2021.
- Bernatchez, P. and Fraser, C.: Evolution of coastal defence structures and consequences for beach width trends, Quebec, Canada, *J. Coast. Res.*, 28(6), 1550–1566, <https://doi.org/10.2112/JCOASTRES-D-10-00189.1>, 2012.
- Björkqvist, J.-V., Lukas, I., Alari, V., van Vledder, G. P., Hulst, S., Pettersson, H., Behrens, A., and Männik, A.: Comparing  
675 a 41-year model hindcast with decades of wave measurements from the Baltic Sea, *Ocean Eng.*, 152, 57–71, <https://doi.org/10.1016/j.oceaneng.2018.01.048>, 2018.
- Booij, N., Ris, R. C., and Holthuijsen, L. H.: A third-generation wave model for coastal regions: 1. model description and validation, *J. Geophys. Res.-Oceans*, 104(C4), 7649–7666. <https://doi.org/10.1029/98JC02622>, 1999.
- Bulleri, F. and Chapman, M.G.: The introduction of coastal infrastructure as a driver of change in marine environments, *J.*  
680 *Appl. Ecol.* 47(1), 26–35. <https://doi.org/10.1111/j.1365-2664.2009.01751.x>, 2010.
- Cappucci, S., Bertoni, D., Cipriani, L. E., Boninsegni, G., and Sarti, G.: Assessment of the anthropogenic sediment budget of a littoral cell system (Northern Tuscany, Italy), *Water*, 12(11), <https://doi.org/10.3390/w1211324>, 2020.
- Eberhardts, G., Grine, I., Lapinskis, J., Purgalis, I., Saltupe, B., and Torklere, A.: Changes in Latvia's seacoast (1935-2007). *Baltica*, 22(1), 11–22, 2009.
- 685 Eelsalu, M., Org, M., and Soomere, T.: Visually observed wave climate in the Gulf of Riga, in: The 6th IEEE/OES Baltic Symposium Measuring and Modeling of Multi-Scale Interactions in the Marine Environment, May 26–29, 2014, Tallinn Estonia, IEEE Conference Publications, <https://doi.org/10.1109/BALTIC.2014.6887829>, 2014.
- Eelsalu, M., Parnell, K. E., and Soomere, T.: Sandy beach evolution in the low-energy microtidal Baltic Sea: attribution of changes to hydrometeorological forcing, *Geomorphology*, 414, 108383,  
690 <https://doi.org/10.1016/j.geomorph.2022.108383>, 2022.
- Eelsalu, M., Viigand, K., and Soomere, T.: Quantification of sediment budget in extensively developed urban areas: a case study of Tallinn Bay, the Baltic Sea, *Regional Studies in Marine Science*, 67, 103199, <https://doi.org/10.1016/j.rsma.2023.103199>, 2023.
- Eelsalu, M., Viigand, K., Soomere, T., and Parnell, K.: Systematic analysis of alongshore sediment transport patterns in  
695 varying sea level conditions for evaluating stability of the coastal areas in the microtidal Baltic Sea, *J. Coast. Res.*, Special Issue 113, 53–57. <https://doi.org/10.2112/JCR-SI113-011.1>, 2024a.



- Eelsalu, M., Soomere, T., and Jankowski, M. Z.: Climate change driven alongshore variations of directional forcing of sediment transport on the eastern Baltic Sea coast, *J. Coast. Res., Special Issue* 113, 256–260, <https://doi.org/10.2112/JCR-SI113-051.1>, 2024b.
- 700 Giudici, A., Jankowski, M. Z., Männikus, R., Najafzadeh, F., Suursaar, Ü., and Soomere, T.: A comparison of Baltic Sea wave properties simulated using two modelled wind data sets. *Estuar. Coast. Shelf Sci.*, 290, 108401, <https://doi.org/10.1016/j.ecss.2023.108401>, 2023.
- Harff, J., Deng, J. J., Dudzinska-Nowak, J., Fröhle, P., Groh, A., Hünicke, B., Soomere, T., and Zhang, W. Y.: What determines the change of coastlines in the Baltic Sea?, in: *Coastline Changes of the Baltic Sea from South to East: Past and Future Projection*, edited by: Harff, J., Furmańczyk, K. and von Storch, H., Coastal Research Library, 19, 15–35, 705 [https://doi.org/10.1007/978-3-319-49894-2\\_2](https://doi.org/10.1007/978-3-319-49894-2_2), 2017.
- Hersbach, H., Bell, B., Berrisford, P., Hirahara, S., Horanyi, A., Muñoz-Sabater, J., Nicolas, J., Peubey, C., Radu, R., Schepers, D., Simmons, A., Soci, C., Abdalla, S., Abellan, X., Balsamo, G., Bechtold, P., Biavati, G., Bidlot, J., Bonavita, M., De Chiara, G., Dahlgren, P., Dee, D., Diamantakis, M., Dragani, R., Flemming, J., Forbes, R., Fuentes, M., 710 Geer, A., Haimberger, L., Healy, S., Hogan, R. J., Holm, E., Janiskova, M., Keeley, S., Laloyaux, P., Lopez, P., Lupu, C., Radnoti, G., de Rosnay, P., Rozum, I., Vamborg, F., Villaume, S., and Thepaut, J. N.: The ERA5 global reanalysis, *Q. J. Roy. Meteor. Soc.*, 146(730), 1999–2049, <https://doi.org/10.1002/qj.3803>, 2020.
- Karpin, V., Heinsalu, A., Ojala, A. E. K., and Virtasalo, J.: Offshore murtoos indicate warm-based Fennoscandian ice-sheet conditions during the Bølling warming in the northern Gulf of Riga, Baltic Sea, *Geomorphology*, 430, 108655, 715 <https://doi.org/10.1016/j.geomorph.2023.108655>, 2023.
- Kinsela, M. A., Morris, B. D., Linklater, M., and Hanslow, D.J.: Second-pass assessment of potential exposure to shoreline change in new south Wales, Australia, using sediment compartments framework, *J. Mar. Sci. Eng.* 5(4), 61. <https://doi.org/10.3390/jmse5040061>, 2017.
- Knaps, R.J.: Sediment transport near the coasts of the Eastern Baltic, in: *Development of sea shores under the conditions of oscillations of the Earth's crust*, Valgus, Tallinn, 21–29, 1966 (in Russian).
- Larson, M., Hoan, L. X., and Hanson, H.: Direct formula to compute wave height and angle at incipient breaking, *J. Waterw. Port C Div.*, 136, 119–122, [https://doi.org/10.1061/\(ASCE\)WW.1943-5460.0000030](https://doi.org/10.1061/(ASCE)WW.1943-5460.0000030), 2010.
- Lentz, S. and Raubenheimer, B.: Field observations of wave setup, *J. Geophys. Res.-Oceans*, 104, 867–875, <https://doi.org/10.1029/1999JC900239>, 1999.
- 725 Leppäranta, M. and Myrberg, K.: *Physical Oceanography of the Baltic Sea*; Springer Science & Business Media, Praxis, Berlin, Heidelberg, <https://doi.org/10.1007/978-3-540-79703-6>, 2009.
- Männikus, R., Soomere, T., and Kudryavtseva, N.: Identification of mechanisms that drive water level extremes from in situ measurements in the Gulf of Riga during 1961–2017, *Cont. Shelf Res.*, 182, 22–36, <https://doi.org/10.1016/j.csr.2019.05.014>, 2019.





- 730 Najafzadeh, F., Jankowski, M. Z., Giudici, A., Männikus, A., Suursaar, Ü., Viška, M., and Soomere, T.: Spatiotemporal variability of wave climate in the Gulf of Riga, *Oceanologia*, 66(1), 56–77, <https://doi.org/10.1016/j.oceano.2023.11.001>, 2024.
- Power, H. E., Hughes, M. G., Aagaard, and T., Baldock, T. E.: Nearshore wave height variation in unsaturated surf, *J. Geophys. Res.-Oceans*, 115, C08030, <https://doi.org/10.1029/2009JC005758>, 2010.
- 735 Raubenheimer, B., Guza, R. T., and Elgar, S.: Wave transformation across the inner surf zone, *J. Geophys. Res.-Oceans*, 101, 25589–25597, <https://doi.org/10.1029/96JC02433>, 1996.
- Raubenheimer, B., Guza, R. T., and Elgar, S.: Field observations of set-down and set-up, *J. Geophys. Res.-Oceans*, 106, 4629–4638, <https://doi.org/10.1029/2000JC000572>, 2001.
- Różyński, G.: Coastal protection challenges after heavy storms on the Polish coast, *Cont. Shelf Res.*, 266, 105080, <https://doi.org/10.1016/j.csr.2023.105080>, 2023.
- 740 Sallenger, A. H. and Holman, R. A.: Wave energy saturation on a natural beach of variable slope, *J. Geophys. Res.-Oceans*, 90, 11939–11944, <https://doi.org/10.1029/JC090iC06p11939>, 1985.
- Skudra, M. and Lips, U.: Characteristics and inter-annual changes in temperature, salinity and density distribution in the Gulf of Riga, *Oceanologia*, 59(1), 37–48. <https://doi.org/10.1016/j.oceano.2016.07.001>, 2017.
- 745 Soomere, T.: Anisotropy of wind and wave regimes in the Baltic proper, *J. Sea Res.*, 49(4), 305–316, [https://doi.org/10.1016/S1385-1101\(03\)00034-0](https://doi.org/10.1016/S1385-1101(03)00034-0), 2003.
- Soomere, T. and Eelsalu, M.: On the wave energy potential along the eastern Baltic Sea coast, *Renew. Energ.*, 71, 221–233, <https://doi.org/10.1016/j.renene.2014.05.025>, 2014.
- Soomere, T. and Viška, M.: Simulated sediment transport along the eastern coast of the Baltic Sea, *J. Mar. Syst.*, 129, 96–105, <https://doi.org/10.1016/j.jmarsys.2013.02.001>, 2014.
- 750 Soomere, T., Bishop, S. R., Viška, M., and Räämet, A.: An abrupt change in winds that may radically affect the coasts and deep sections of the Baltic Sea, *Clim. Res.*, 62, 163–171, <https://doi.org/10.3354/cr01269>, 2015.
- Soomere, T., Männikus, R., Pindsoo, K., Kudryavtseva, N., and Eelsalu, M.: Modification of closure depths by synchronisation of severe seas and high water levels, *Geo-Mar. Lett.*, 37(1), 35–46, <https://doi.org/10.1016/10.1007/s00367-016-0471-5>, 2017.
- 755 Soomere, T., Eelsalu, M., Viigand, K., and Giudici, A.: Linking changes in the directional distribution of moderate and strong winds with changes in wave properties in the eastern Baltic proper, *J. Coast. Res.*, Special Issue 113, 190–194. <https://doi.org/10.2112/JCR-SI113-038.1>, 2024.
- Susilowati, Y., Nur, W. H., Sulaiman, A., Kumoro, Y., and Yunarto: Study of dynamics of coastal sediment cell boundary in Cirebon coastal area based on integrated shoreline Montecarlo model and remote sensing data, *Regional Studies in Marine Science*, 52, 102268. <https://doi.org/10.1016/j.rsma.2022.102268>, 2022.
- 760 Suursaar, Ü., Kullas, T., and Otsmann, M.: A model study of the sea level variations in the Gulf of Riga and the Väinameri Sea, *Cont. Shelf Res.* 22(14), 2001–2019, [https://doi.org/10.1016/S0278-4343\(02\)00046-8](https://doi.org/10.1016/S0278-4343(02)00046-8), 2002.



- 765 Thom, B. G., Eliot, I., Eliot, M., Harvey, N., Rissik, D., Sharples, C., Short, A. D., and Woodroffe, C. D.: National sediment  
compartment framework for Australian coastal management, *Ocean Coast. Manage.*, 154, 103–120.  
<https://doi.org/10.1016/j.ocecoaman.2018.01.001>, 2018.
- 770 Tõnisson, H., Suursaar, Ü., Alari, V., Muru, M., Ravis, R., Kont, A., and Viitak, M.: Measurement and model simulations of  
hydrodynamic parameters, observations of coastal changes and experiments with indicator sediments to analyse the  
impact of storm St. Jude in October, 2013, *J. Coast. Res., Special Issue 75*, 1257–1261, <https://doi.org/10.2112/SI75-25>,  
2016.
- Tsyrlunikov, A., Tuuling, I., and Hang T.: Streamlined topographical features in and around the Gulf of Riga as evidence of  
Late Weichselian glacial dynamics. *Geol. Quart.*, 52(1), 81–89, 2008.
- Ulsts, V.: *Latvian coastal zone of the Baltic Sea (In Latvian)*, 1998.
- 775 USACE: *Coastal Engineering Manual*. Department of the Army. U.S. Army Corps of Engineers. Manual No. 1110-2-1100,  
2002.
- Villasante, S., Richter, K., Bailey, J., Blenckner, T., Farrell, E., Mongruel, R., Timmermann, K., Bouma, T., Melaku Canu,  
D., Chen, M., Lachs, L., Payo, A., and Sousa Pinto, I.: *Building Coastal Resilience in Europe*, edited by Alexander, B.,  
Muñiz Piniella, A., Kellett, P., Rodriguez Perez, A., Van Elslander, J., Bayo Ruiz, F., Heymans, J. J., Position Paper 27  
of the European Marine Board, Ostend, Belgium, <https://doi.org/10.5281/zenodo.8224055>, 2023.
- 780 Viška, M. and Soomere, T.: Long-term variations of simulated sediment transport along the eastern Baltic Sea coast as a  
possible indicator of climate change, in: *7th Study Conference on BALTEX*, 10–14 June 2013, Borgholm, Island of  
Öland, Sweden, Conference Proceedings, edited by Reckermann, M. and Köppen, S., International BALTEX Secretariat,  
Publication No. 53, 99–100, 2013a.
- 785 Viška, M. and Soomere, T.: Simulated and observed reversals of wave-driven alongshore sediment transport at the eastern  
Baltic Sea coast, *Baltica*, 26(2), 145–156, <https://doi.org/10.5200/baltica.2013.26.15>, 2013b.